

Suppressing Aeroelastic Vibrations via Stability Region Maximization and Numerical Continuation Techniques

Max Demenkov* Mikhail Goman**

* Faculty of Computing Sciences and Engineering, De Montfort University, Queens bld. 2.14, The Gateway, Leicester LE1 9BH, UK
(e-mail: demenkov@dmu.ac.uk)

** Faculty of Computing Sciences and Engineering, De Montfort University, Gateway bld. 6.56, The Gateway, Leicester LE1 9BH, UK
(e-mail: mgoman@dmu.ac.uk)

Abstract: An active flutter suppression using linear sub-optimal control scheme is investigated for a 2dof airfoil system with nonlinear torsional stiffness and limited deflection amplitude of its single actuator. The suppression of limit cycle oscillations in the nonlinear closed-loop system is achieved through maximization of the stability region of its linearized system. The critical value of the control input amplitude is determined via numerical continuation of the closed-loop limit cycle. At this value, the cycle experiences saddle-node bifurcation and disappears, satisfying the necessary condition for the global stability in the closed-loop system.

Keywords: Active vibration control, nonlinear systems, control input constraints, stability regions, bifurcation analysis

1. INTRODUCTION

Active flutter suppression approach has been studied in many papers to prevent catastrophic structural failures due to excessive vibrations in aeroelastic systems. It is expected that a designed feedback stabilizes an unstable aeroelastic system with nonlinear torsional and/or bending stiffness around nominal zero-pitch, zero-plunge equilibrium and delays the onset of the limit cycle oscillations (LCO). The limited control power of aerodynamic surfaces can be, however, insufficient to suppress these oscillations globally.

It is well known that the origin of a closed-loop nonlinear system can be asymptotically stable only in some bounded region in the state-space (called *stability region*, or *region of attraction*). Nonlinear systems may possess many different attractors (such as stable limit cycles) with their own stability regions. The closed-loop system performance can degrade, for example, because of the small stability region of the origin in the presence of LCO. In this case, it is natural to create a feedback that maximizes the stability region of the origin as much as possible in order to delay flutter onset in an aeroelastic system. This approach to the flutter suppression problem was considered in Goman and Demenkov [2004] and Applebaum and Ben-Asher [2007]. In these two papers, aeroelastic systems were represented by linear systems with constrained control inputs and the influence of nonlinear stiffness on the closed-loop system performance was not studied.

Due to the nonlinear nature of aeroelastic systems, it is theoretically possible that with maximization of the closed-loop stability region, the closed-loop limit cycle will

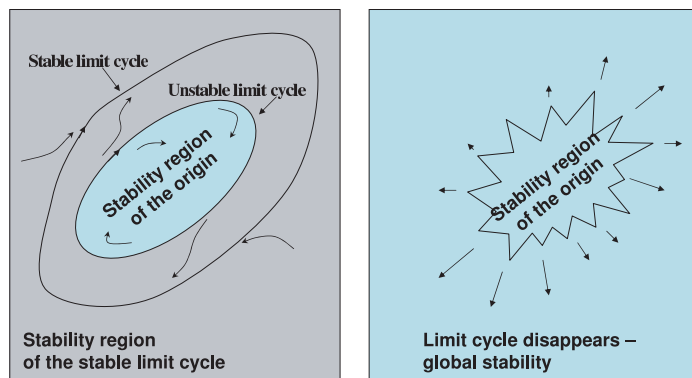


Fig. 1. Stability region maximization for the limit cycle elimination.

disappear. In this case, its stability region will merge with the region of attraction of the origin, resulting in globally stable closed-loop system (see Fig. 1).

In this paper we investigate this scenario using a mathematical model of the aeroelastic apparatus developed in Texas A&M University. In (Ko et al. [1997, 1998], Kurdila et al. [2001], Platanitis and Strganac [2004]) (see also references therein) different approaches were used for controlling the apparatus with amplitude constrained trailing edge actuator. In Platanitis and Strganac [2004] the lead-

ing edge actuator was additionally introduced in order to improve the controllability. Even with two actuators, the LCO prevention was possible only in a limited flow velocity range $V < 17$ m/s.

We show that it is possible to eliminate a stable limit cycle in the closed-loop system with only one (trailing edge) actuator, if we increase the maximum deflection amplitude of the actuator by only 1 deg. The controller is designed using a method that maximizes the stability region of the linearized closed-loop system under amplitude control constraints. It was previously shown (Formalsky [1968], Goman et al. [1996], Hu and Lin [2001]) that even a linear open-loop unstable system with saturated control inputs can be asymptotically stabilized only inside some bounded (*controllable*) region in the state-space. The controller explicitly takes into account the amplitude control constraints, using the method proposed in Goman et al. [1996] and Hu and Lin [2001].

For the post-design nonlinear analysis we employ numerical continuation of the closed-loop limit cycle with the maximum amplitude of a control signal as the continuation parameter. We show that the *saddle-node bifurcation* occurs at some critical value of the actuator amplitude. At this point the closed-loop limit cycle disappears. Although this is not a proof of global stability, it is a necessary condition for that. In this case, our extensive numerical simulations with different initial conditions cannot reveal any other attractors in the closed-loop system that are different from the origin.

2. SYSTEM MODEL

The equations of motion for a wing section with two degrees of freedom (see Fig. 2) are taken here as they were presented in Platanitis and Strganac [2004]:

$$\begin{bmatrix} m_T & m_W x_\alpha b \\ m_W x_\alpha b & I_\alpha \end{bmatrix} \begin{bmatrix} \ddot{h} \\ \ddot{\alpha} \end{bmatrix} + \begin{bmatrix} c_h \dot{h} \\ c_\alpha \dot{\alpha} \end{bmatrix} + \begin{bmatrix} F_h \\ M_\alpha \end{bmatrix} = \begin{bmatrix} -L(t) \\ M(t) \end{bmatrix}, \quad (1)$$

where h - the plunge displacement, α - the pitch angle, m_T - the total mass of pitch-plunge system, m_W - the total wing section plus mount mass, $F_h(h) = k_h h$ - the plunge force due to the plunge stiffness k_h , $M_\alpha(\alpha) = k_\alpha \alpha$ - the pitch moment due to the pitch stiffness k_α . The parameters of the model are given in Table 1.

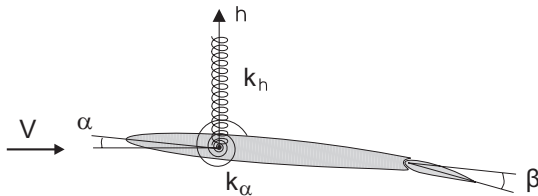


Fig. 2. The 2dof wing section.

It is important to note that the sole source of nonlinearity in these equations arises from the polynomial model of the pitch stiffness:

$$k_\alpha(\alpha) = 12.77 + 53.47\alpha + 1003\alpha^2. \quad (2)$$

Table 1. System parameters

Parameter	Value
ρ	1.225 kg/m ³
a	-0.6719
b	0.1905 m
s	0.5945 m
k_h	2844 N/m
c_h	27.43 kg/s
c_α	0.0360 kg·m ² /s
m_{wing}	4.340 kg
m_W	5.230 kg
m_T	15.57 kg
I_{cam}	0.04697 kg·m ²
$I_{\text{cg-wing}}$	0.04342 kg·m ²
C_{l_α}	6.757
C_{l_β}	3.774
C_{m_β}	-0.6719

Using the nondimensional distance from midchord to elastic axis position a and the semichord of wing section b , we first compute the nondimensional distance from elastic axis to center of mass x_α and then distance r_{cg} :

$$x_\alpha = -(0.0998 + a), r_{\text{cg}} = b x_\alpha. \quad (3)$$

Viscous damping coefficients for plunge and pitch motion are represented in the equations by c_h and c_α , respectively. The total pitch moment of inertia about elastic axis I_α is computed as

$$I_\alpha = I_{\text{cam}} + I_{\text{cg-wing}} + m_{\text{wing}} r_{\text{cg}}^2, \quad (4)$$

where I_{cam} - the pitch cam moment of inertia, $I_{\text{cg-wing}}$ - the wing section moment of inertia about the center of gravity, m_{wing} - the mass of wing section.

We assume that the quasi-steady aerodynamic force L and moment M are modelled as

$$L = \rho V^2 b s \{ C_{l_\alpha} [\alpha + (\dot{h}/V) + (1/2 - a)b(\dot{\alpha}/V)] + C_{l_\beta} \beta \}, \quad (5)$$

$$M = \rho V^2 b^2 s \{ C_{m_\alpha - \text{eff}} [\alpha + (\dot{h}/V) + (1/2 - a)b(\dot{\alpha}/V)] + C_{m_\beta - \text{eff}} \beta \},$$

where ρ - the air density, V - the freestream velocity, s - the wing section span, β - the trailing-edge control surface deflection.

The effective dynamic and control moment derivatives due to angle of attack ($C_{m_\alpha - \text{eff}}$) and trailing-edge control surface deflection $C_{m_\beta - \text{eff}}$ about the elastic axis are defined as follows:

$$\begin{aligned} C_{m_\alpha - \text{eff}} &= (1/2 + a)C_{l_\alpha} + 2C_{m_\alpha}, \\ C_{m_\beta - \text{eff}} &= (1/2 + a)C_{l_\beta} + 2C_{m_\beta}, \end{aligned} \quad (6)$$

where $C_{l_{\alpha,\beta}}$ - lift and $C_{m_{\alpha,\beta}}$ - moment coefficients per angle of attack and control surface deflections, respectively. Note that $C_{m_\alpha} = 0$ for a symmetric airfoil, as in our case.

Let us write the system in the following form:

$$F\ddot{y} + G\dot{y} + C(\alpha)y = Du \quad (7)$$

where

$$\begin{aligned}
y &= \begin{bmatrix} h \\ \alpha \end{bmatrix}, u = \beta \frac{180}{\pi}, F = \begin{bmatrix} m_T & m_W x_\alpha b \\ m_W x_\alpha b & I_\alpha \end{bmatrix}, \\
G &= \begin{bmatrix} c_h + \rho V b s C_{l_\alpha} & \rho V b^2 s C_{l_\alpha} (1/2 - a) \\ -\rho V b^2 s C_{m_\alpha - \text{eff}} & c_\alpha - \rho V b^3 s C_{m_\alpha - \text{eff}} (1/2 - a) \end{bmatrix}, \\
C(\alpha) &= \begin{bmatrix} k_h & \rho V^2 b s C_{l_\alpha} \\ 0 & k_\alpha(\alpha) - \rho V^2 b^2 s C_{m_\alpha - \text{eff}} \end{bmatrix}, \\
D &= \frac{\pi}{180} \begin{bmatrix} -\rho V^2 b s C_{l_\beta} \\ \rho V^2 b^2 s C_{m_\beta - \text{eff}} \end{bmatrix}.
\end{aligned} \tag{8}$$

All state variables in this model are in radians and radians per second, while the control u is in degrees.

Now it is easy to write the system in the Cauchy form:

$$\begin{aligned}
\begin{bmatrix} \dot{y} \\ \ddot{y} \end{bmatrix} &= \begin{bmatrix} 0_{2 \times 2} & E_{2 \times 2} \\ -F^{-1}C(\alpha) & -F^{-1}G \end{bmatrix} \begin{bmatrix} y \\ \dot{y} \end{bmatrix} + \\
\begin{bmatrix} 0 \\ 0 \\ F^{-1}D \end{bmatrix} u &= A(x)x + bu,
\end{aligned} \tag{9}$$

where

$$x = \begin{bmatrix} y \\ \dot{y} \end{bmatrix}, 0_{2 \times 2} = \begin{bmatrix} 0 & 0 \\ 0 & 0 \end{bmatrix}, E_{2 \times 2} = \begin{bmatrix} 1 & 0 \\ 0 & 1 \end{bmatrix}.$$

The actuator deflection u is subject to the amplitude constraints: $|u| \leq u_{max}$. At the flutter speed $V_{flat} = 11.4 \text{ m/s}$ the limit cycle appears in the open-loop system (i.e. with $u = 0$) and remains for the subsequent velocity values (see Fig. 3).

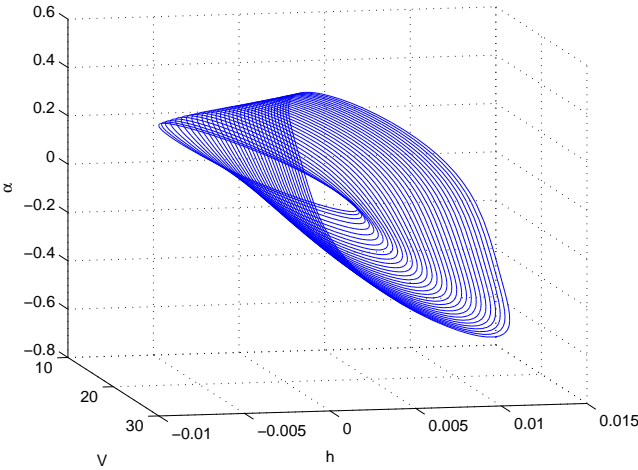


Fig. 3. Open-loop limit cycles for $V=12-30 \text{ m/s}$.

3. MAXIMUM STABILITY REGION DESIGN FOR THE LINEAR CONSTRAINED SYSTEM

Let us consider the following open-loop unstable continuous-time system:

$$\dot{x}(t) = Ax(t) + bu(t) \tag{10}$$

where q eigenvalues of $A \in R^{n \times n}$ have positive real parts and others are stable, $b \in R^{n \times 1}$, $x \in R^n$ and $u \in R^1$.

The state vector x is fully observable. This system can be derived from the nonlinear model (9) if one takes A as the linearization of $A(x)$ at $\alpha = 0$ and $V > V_{flat}$.

We will use the following saturation function to satisfy amplitude control constraints:

$$\text{sat}(u) = \text{sign}(u) \min\{u_{max}, |u|\}. \tag{11}$$

While the stability of an equilibrium in a linear system is a global property, the stability of an equilibrium in a nonlinear system is just a local characteristic. The unstable linear system in (10) under any control law with constrained input becomes nonlinear and can be stable only in a bounded region of the state-space, known as *stability region* or *region of attraction*. The maximum attainable region of attraction coincides with the *controllable region*, which is also called the *asymptotically null controllable region* (Formalsky [1968], Goman et al. [1996], Hu and Lin [2001], Demenkov [2006]).

To reduce the system dimension while synthesizing the controller, it is natural to take into account only the subspace corresponding to the unstable eigenvalues. There are two widely known state transformations that we can use for this purpose: the first one is based on the Schur decomposition (Castelan et al. [1996], Golub and Loan [1986]) of the system matrix A and the second one is based on the block Jordan decomposition of the matrix A . We will use the Schur decomposition as the most robust and reliable, even in the case of multiple and defective eigenvalues.

Let us suppose that in general case n system matrix eigenvalues are arranged in a list in increasing order of their real parts with the first $n - q$ stable eigenvalues and the last q unstable ones. The stable eigenvalues are placed in the beginning of the list. Consider the following transformation of basis in (10):

$$x = [Q_1|Q_2] \begin{bmatrix} s \\ z \end{bmatrix} \tag{12}$$

where the matrix $Q = [Q_1|Q_2]$ is orthogonal ($Q^T Q = I$) and such that the columns of $Q_1 \in R^{n \times (n-q)}$ and $Q_2 \in R^{n \times q}$ span the subspaces associated with the stable and unstable eigenvalues, respectively. This matrix can be obtained from the Schur decomposition of matrix A by reordering, if necessary, eigenvalues of its diagonal blocks (Golub and Loan [1986]) in accordance with the eigenvalue list formed.

In the new basis the open-loop system is represented by

$$\begin{bmatrix} \dot{s}(t) \\ \dot{z}(t) \end{bmatrix} = Q^T A Q \begin{bmatrix} s(t) \\ z(t) \end{bmatrix} + Q^T b u(t) = \tag{13}$$

$$\begin{bmatrix} A_{11} & A_{12} \\ 0 & A_z \end{bmatrix} \begin{bmatrix} s(t) \\ z(t) \end{bmatrix} + \begin{bmatrix} b_1 \\ b_z \end{bmatrix} u(t)$$

where the eigenvalues of matrices A_{11} and A_z contain the stable and unstable ones, respectively.

Note that the dynamics of $z(t)$ associated with the unstable eigenvalues is decoupled from $s(t)$. Thus we can isolate the following open-loop reduced-order subsystem:

$$\dot{z}(t) = A_z z(t) + b_z u(t), \tag{14}$$

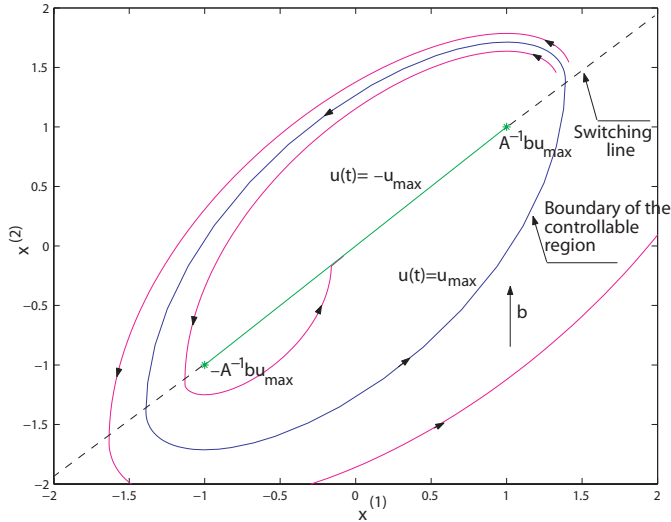


Fig. 4. An example of system with "stability optimal" relay control law: zone of the sliding mode is depicted by green color.

where $A_z \in R^{q \times q}$, $b_z \in R^{q \times 1}$ and $z(t) = Q_2^T x(t)$. If the state of system (14) is kept in its equilibrium point with $z(t) = 0$ and $u(t) = 0$, it is trivial to show that $s(t)$ asymptotically tends to the origin and thus we need to stabilize only subsystem (14).

From the previous studies of the considered aeroelastic system (Ko et al. [1997, 1998], Kurdila et al. [2001], Platanitis and Strganac [2004]) it is well known that in our case the unstable subsystem is two-dimensional. Therefore, we need to stabilize only this two-dimensional subsystem so that to maximize its stability region as much as possible. This will mean maximization of the stability region for the whole system as well.

A simple solution to this problem has been proposed in Goman et al. [1996], where the optimal control law is the relay-type ($u(t) = \pm u_{max}$) and specified by a switching line. Two equilibrium points $z_{eq} = \pm A_z^{-1} b_z u_{max}$ are positioned on this line, which is derived geometrically using nonlinear dynamics analysis (see Fig. 4). The stability region in this case is bounded by the limit cycle semi-curves. A sliding mode zone is situated on the switching line between the equilibrium points.

In Hu and Lin [2001] this result was rediscovered from the different viewpoint. It was established that for the considered class of systems the linear quadratic (LQ) optimal controller provides the system with a domain of attraction, which approaches the controllable region as the feedback gain increases towards infinity. In the last case, the relay-type "stability optimal" control law tends to be exactly the same as the controller proposed in Goman et al. [1996].

Let P be the unique positive definite solution to the following algebraic Riccati equation:

$$A_z^T P + P A_z - P^T b_z b_z^T P = 0 \quad (15)$$

Note that this equation is associated with the minimum energy regulation, i.e., an LQ problem with the cost func-

tion $J = \int_0^\infty u^T(t)u(t)dt$. The corresponding minimum energy state feedback gain is given by

$$K = -b_z^T P.$$

It is known that in a linear system (without constraints) under LQ control the feedback gain can be increased indefinitely without loss of stability. The result stated in Hu and Lin [2001] is that for the saturated feedback law

$$u(t) = \text{sat}(\gamma K z)$$

the domain of attraction will approach the controllable region as $\gamma \rightarrow \infty$.

In this paper, we use this LQ-based approach to compute sub-optimal control law with stability region large enough to eliminate the stable limit cycle in the closed-loop nonlinear system. To compute this control law in MATLAB, we perform the Schur decomposition of the system and then apply LQ synthesis with the given parameter γ to obtain feedback gain K :

```
function K=StabOpt(A,b,gamma)
n=size(A,1);
stable=length(find(real(eig(A))<0));
if stable==0
    % Stabilize the whole system
    K=-gamma*lqr(A,b,zeros(n,n),1);
elseif stable<n
    % Perform Schur decomposition
    unst=n-stable;
    [Q,QAQ]=schur(A);
    [Q,QAQ]=ordschur(Q,QAQ,'lhp');
    Q_2=Q(:,end-unst+1:end);
    Qb=Q'*b;
    Az=QAQ(end-unst+1:end,end-unst+1:end);
    bz=Qb(end-unst+1:end);
    % Apply Tingshu Hu theorem
    Kz=-lqr(Az,bz,zeros(unst,unst),1);
    % z=Q_2'*x - transformation into
    % the unstable subspace
    K=gamma*Kz*Q_2';
else
    % All eigenvalues are stable -> do nothing
    K=zeros(1,n);
end
```

4. BIFURCATION ANALYSIS OF THE CLOSED-LOOP SYSTEM

Bifurcation analysis (Kuznetsov [2004]) via numerical continuation is a well developed area (Allgower and Georg [1990]). Various numerical continuation software tools have been developed, such as the famous AUTO or KRIT, which was tailored for the aerospace applications (Goman et al. [1997]), as well as Matlab toolbox MATCONT (Govaerts et al. [2003]). The main purpose of the numerical continuation is to trace an invariant manifold (e.g. equilibrium or limit cycle) of a nonlinear system. A software package computes the corresponding manifold versus the continuation parameter, selected by the user, and detects its stability and bifurcations along the solution curve.

A limit cycle and its bifurcations generally can be traced via a fixed point of a Poincare mapping, computed as the intersection of a smooth hypersurface with the limit cycle

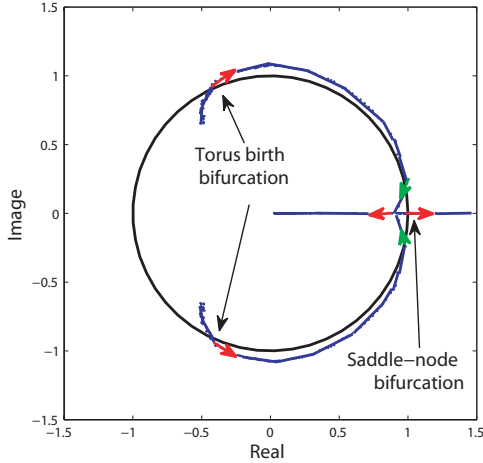


Fig. 5. Multipliers for the closed-loop cycles.

(one can see a diagram constructed from such intersections in Fig. 7). The Floquet multipliers are also calculated. They are the eigenvalues of the corresponding *monodromy* matrix, which is in turn the local linearization of the Poincare mapping evaluated at the fixed point. We need Floquet multipliers to confirm the presence of both stable and unstable limit cycles near bifurcation points.

For continuation of limit cycles in the closed-loop system we use the software package MATCONT. The saturation function (11) is actually non-smooth and not very suitable for numerical algorithms implemented in the package. In our analysis we smoothed the saturation function by "inserting" a circle with some radius into the corners of the saturation characteristic.

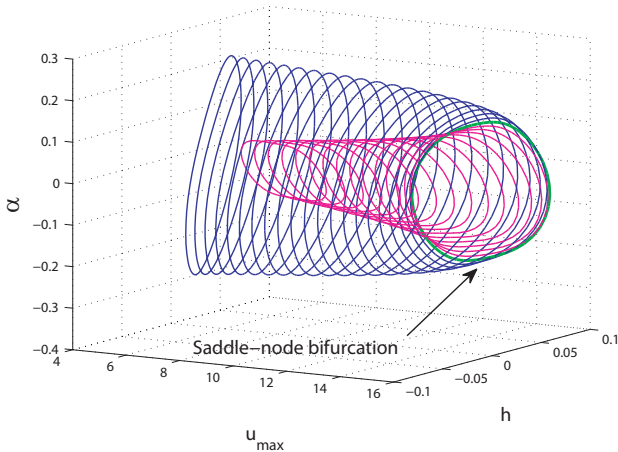


Fig. 6. Closed-loop stable (blue) and unstable (red) limit cycles vs. u_{max} for $V = 25$ m/s.

We take u_{max} as the continuation parameter and start our continuation at $u_{max} = 6$ deg, $V = 25$ m/s from the stable limit cycle, which was initially computed via direct simulation (see Fig. 6). For the controller synthesis we assume that $\gamma = 2$. Although this value does not give us the maximum stability region, it is a good compromise between stability region size and the size of linear zone around the origin. The small size of this zone leads to the

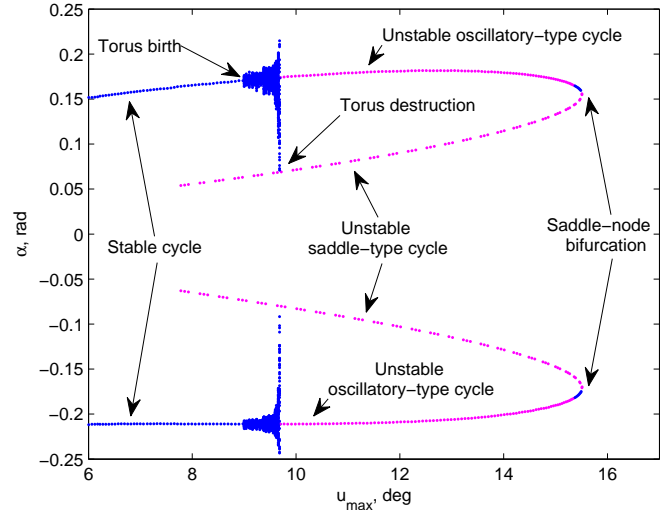


Fig. 7. Bifurcation diagram with Poincare plane $h = 0$ for $V = 25$ m/s.

relay-type control and affects the numerical robustness of algorithms implemented in MATCONT.

The numerical continuation reveals that the *saddle-node (or fold) bifurcation* (Kuznetsov [2004]) occurs at some u_{crit} between $u_{max} = 15$ and 16 degrees. The bifurcation scenario implies the collision and disappearance of two limit cycles, the stable one and the unstable one of saddle-type. The unstable cycle has one multiplier of its Poincare mapping situated outside the unit circle in the complex plane.

Being initially stable at small u_{max} , the closed-loop limit cycle first loses its stability after the *torus birth* via the Neimark-Sacker bifurcation (see Fig. 7) and then, after the second Neimark-Sacker bifurcation, regains stability in a very short range of u_{max} before its final disappearance. As one can see in Fig. 6, two limit cycles, stable one (blue) and unstable one of saddle-type (red) really collide and disappear in the closed-loop system at $u_{max} = u_{crit}$. The analysis of the Floquet multipliers (Fig. 5) confirms the required stable and saddle stability properties. The torus birth and its destruction, leading to destabilization of LCO, is described with more details in Goman and Demenkov [2008].

Investigation of the bifurcation values u_{max} for the flow velocity range $V = 11 - 30$ m/s reveals that the fold bifurcation occurs always at $u_{crit} < 16$ deg. Note that in Platanitis and Strganac [2004] the amplitude control constraint was assumed to be equal 15 deg. Therefore, to destroy the limit cycle by means of the considered saturated linear controller far beyond 17 m/s, we need to increase maximum actuator amplitude by only *one degree*.

The numerical simulation of the closed-loop nonlinear system confirms the disappearance of the limit cycles in the closed-loop system after $u_{max} = 16$ deg. Based on extensive simulation results with different initial conditions taken on a fine grid of equidistant points in (α, h) -plane, the system is asymptotically stable in the considered flow velocity range $V = 11 - 30$ m/s (see an example

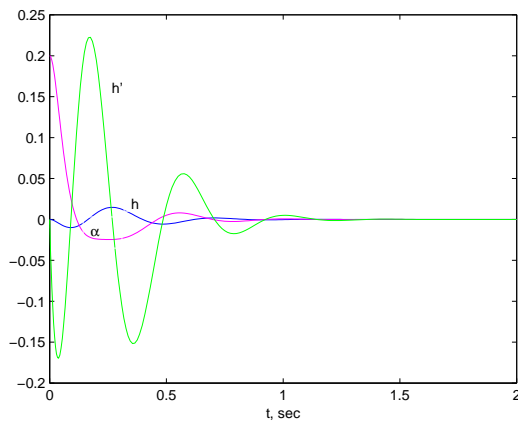


Fig. 8. State variables α, h, \dot{h} for $V = 30$ m/s.

in Fig. 8). However, the numerical simulations by itself cannot guarantee the global stability of the closed-loop system, therefore, further theoretical confirmation is required.

5. CONCLUSIONS

A sub-optimal controller maximizing the stability region of the linearized system with bounded amplitude of control input was successfully applied to suppress limit cycle oscillations in an aeroelastic system with nonlinear torsional stiffness. For the validation of the proposed controller, the continuation technique was applied for investigation of the closed-loop system limit cycle at different levels of the control input constraint. This analysis shows the existence of some critical value for maximum control amplitude, at which stable and unstable limit cycles merge and disappear through the fold bifurcation. The main result of this paper is the proposed feedback synthesis methodology. It consists of the synthesis of a sub-optimal linear saturated regulator plus post-design bifurcation analysis and identification of the minimum level of control constraint leading to the elimination of the limit cycle. This methodology can be applicable to the vibration suppression in other nonlinear systems.

REFERENCES

- E.L. Allgower and K. Georg. *Numerical Continuation Methods: an Introduction*. Springer-Verlag, New York, 1990.
- E. Applebaum and J.Z. Ben-Asher. Control of an aeroelastic system with actuator saturation. *Journal of Guidance, Control, and Dynamics*, 30(2):548–556, 2007.
- E.B. Castelan, J.M. Gomes da Silva Jr., and J.E.R. Cury. A reduced-order framework applied to linear systems with constrained controls. *IEEE Transactions on Automatic Control*, 41:249–255, 1996.
- M. Demenkov. Stability-optimal control for planar unstable systems. In *Proceedings of the UKACC International Control Conference*, Glasgow, UK, August 2006.
- A.M. Formalsky. Controllability domain of systems having limited control resources. *Automation and Remote Control*, 29(3):375–382, 1968.
- G.H. Golub and C.F. Van Loan. *Matrix computations*. North Oxford Academic publ., London, 1986.
- M. Goman, E. Fedulova, and A. Khramtsovsky. Maximum stability region design for unstable aircraft with control constraints. In *AIAA Guidance, Navigation and Control Conference Proceedings*, San Diego, California, July 1996. AIAA Paper 96-3910.
- M.G. Goman and M.N. Demenkov. Multiple attractor dynamics in active flutter suppression problem. In *ICNPAA 2008: Mathematical Problems in Engineering, Aerospace and Sciences*, Genoa, Italy, June 2008.
- M.G. Goman and M.N. Demenkov. Computation of controllability regions for unstable aircraft dynamics. *AIAA Journal of Guidance, Control and Dynamics*, 27: 647–656, 2004.
- M.G. Goman, G.I. Zagainov, and A.V. Khramtsovsky. Application of bifurcation methods to nonlinear flight dynamics problems. *Progress in Aerospace Sciences*, 33: 539–586, 1997.
- W. Govaerts, A. Dhooge, and Y.A. Kuznetsov. Matcont: a matlab package for numerical bifurcation of odes. *ACM Transactions on Mathematical Software*, 29:141–164, 2003.
- T. Hu and Z. Lin. *Control Systems with Actuator Saturation: Analysis and Design*. Birkhäuser, Boston, 2001.
- J. Ko, A.J. Kurdila, and T.W. Strganac. Nonlinear control of a prototypical wing section with torsional nonlinearity. *Journal of Guidance, Control, and Dynamics*, 20(6): 1181–1189, 1997.
- J. Ko, T.W. Strganac, and A.J. Kurdila. Stability and control of a structurally nonlinear aeroelastic system. *Journal of Guidance, Control, and Dynamics*, 21(5): 718–725, 1998.
- A.J. Kurdila, T.W. Strganac, J.L. Junkins, J. Ko, and M.R. Akella. Nonlinear control methods for high-energy limit-cycle oscillations. *Journal of Guidance, Control, and Dynamics*, 24(1):185–192, 2001.
- Y.A. Kuznetsov. *Elements of Applied Bifurcation Theory*. Springer, New York, 2004.
- G. Platanitis and T.W. Strganac. Control of a nonlinear wing section using leading- and trailing-edge surfaces. *Journal of Guidance, Control, and Dynamics*, 27(1):52–58, 2004.